Two-pion correlations and multiplicity effects in La on La collisions

H. Bossy, J. A. Bistirlich, R. R. Bossingham, A. D. Chacon,* K. M. Crowe, Y. Dardenne, M. Justice, J. O. Rasmussen, A. A. Shihab-Eldin, M. A. Stoyer,† and K. D. Wyatt

Lawrence Berkeley Laboratory, University of California, Berkeley, California 94720

J. P. Sullivan‡ and K. L. Wolf

Cyclotron Institute, Texas A&M University, College Station, Texas 77843

(Received 10 December 1991; revised manuscript received 30 November 1992)

Bose-Einstein correlations of negative pions in heavy ion collisions have been investigated for the reaction ^{139}La + ^{nat}La $\rightarrow 2\pi^- + X$ at 1.26 GeV/nucleon at two acceptances, centered at laboratory observation angles of approximately 0° and 45° with respect to the beam axis. A scintillation counter array downstream of the target was used to sample the charged particle multiplicity of each event and hence give some information on the impact parameter of the collision. Including results from previous experiments, space-time dimensions of the pion source are now available for mass-symmetric collisions in the mass range of $A = 40$ to 139. The sources are oblate for nearly all systems, except for La + La central collisions viewed near 45° in the laboratory (90° in the center of mass) where the source is spherical. The perpendicular radius $R_\perp$ is never less than 4 fm, regardless of the centrality of the La + La collision. Furthermore, $R_\perp$ seems independent of the mass of the collision system.

PACS number(s): 25.75.+r

I. INTRODUCTION

Since the discovery by Goldhaber *et al.* [1, 2] that proton-antiproton annihilations produce more like-charged than oppositely charged pion pairs with small momentum difference, many theoretical [3–20] and experimental [21–36] studies have been done to investigate the "Goldhaber-Goldhaber-Lee-Pais" (GGLP) effect. The correlation of two like particles is a consequence of the quantum mechanical symmetry requirement imposed on the wave functions of bosons. Bose-Einstein correlations were first employed in radio astronomy by Hanbury-Brown *et al.* [37] to measure the size of stellar objects; similarly, Bose-Einstein correlations of pions, kaons, and other particles can be used to determine the space-time dimensions and chaoticity of particle sources (nonchaotic or coherent sources do not show any Bose-Einstein correlation effects [7]). The determination of the dimensions of hadronic sources in heavy ion collisions provides experimental data for the test of transport calculations that treat the complex collision process of a large number of nucleons. By grouping the data according to the charged particle multiplicity it should be possible to measure the space-time dimensions of the particle source as a function of the centrality of the collision. There have been predictions [9, 16] of phase transitions from ordinary nuclear matter to quark-gluon plasma occurring in collisions of highly relativistic nuclei. One probe might be Bose-Einstein correlation measurements [12, 38]. Although it is generally agreed that Bevalac energies are well below the threshold for the quark-gluon plasma phase transition, understanding Bose-Einstein correlations at Bevalac energies is important as a base line for higher-energy work.

II. EXPERIMENT

In this work we continue the systematic investigation of two-pion correlations in symmetric projectile-target systems at the Lawrence Berkeley Laboratory Bevalac with an experiment using a 1.26 GeV/nucleon ^{139}La beam on a ^{nat}La target of 0.5 g/cm^2 thickness. Negative pion pairs were measured with the magnetic spectrometer Janus at angles of 0° and 45° (laboratory) with respect to the beam axis, the latter angle corresponding to approximately 90° in the center-of-mass (c.m.) system. The experimental setup, described in detail by Zajc *et al.* [26] and Chacon *et al.* [36], is shown in Fig. 1. The magnetic fields used are given in Table I. As an addition to the previous setups, an array of 28 scintillation counters (see Fig. 1, inset) was mounted 363 cm downstream of the 45° target position to give some measure of the impact parameter of each event. When taking the 0° data, the downstream scintillator array was shifted laterally by

*Present address: Cyclotron Institute, Texas A & M University, College Station, TX 77843.

†Present address: MS L–234, University of California, P. O. Box 808, Lawrence Livermore National Laboratory Livermore, CA 94550.

‡Present address: P2 Division, MS D456, Los Alamos National Laboratory, Los Alamos, NM 87545.

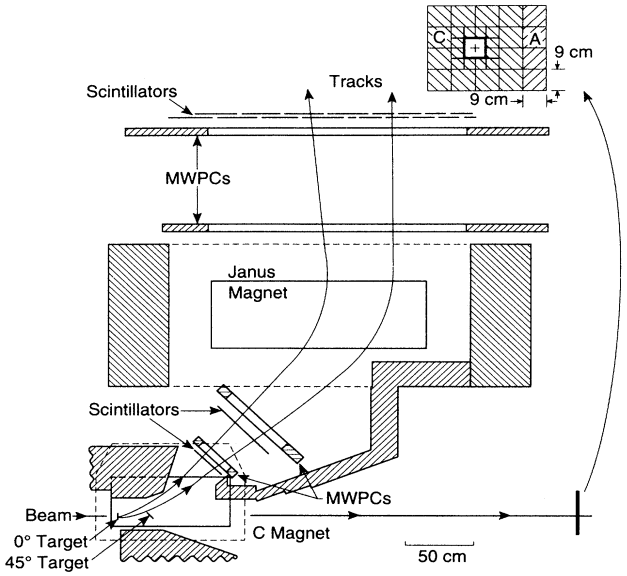

FIG. 1. Top view of the experimental setup. Inset: front view of the multiplicity counter array with central scintillators (labeled "C") and peripheral scintillators ("A").

27 cm to compensate for beam steering by the C-magnet, so that the beam was always centered on the array. The gain of the photomultiplier tubes was adjusted to measure protons and light charged fragments. The attempt to detect beam particles and heavy residues with the innermost counters was not successful due to high counting rates and excessive radiation damage to the scintillators. Therefore, these counters were excluded from the final analysis. This gives a hollow rectangular array with an average angular detection range from 0.80° to 3.61° for area "C" and 3.61° to 5.41° for area "A," in the 45° setup (see Fig. 1, inset). The electronic event trigger was the same as in previous experiments [30, 36]. That is, the coincidence condition requires (1) a coincidence signal from the two scintillation counters before the Janus magnet, (2) two separated hits in the two-plane scintillator array after the magnet, and (3) the prompt signal from the tracking wire chambers [36]. This trigger effectively selected those events where two negative particles had passed through the spectrometer. Time and pulse-height signals of each multiplicity counter were recorded for each event.

III. ANALYSIS

Assuming a Gaussian space-time source distribution with radii perpendicular to the beam direction $R_\perp$, a radius parallel to the beam direction $R_\parallel$, a lifetime τ, and a chaoticity parameter λ, the following correlation function was fit to the data:

$$C(q_\perp, q_\parallel, q_0) = B[1+\lambda \exp\{(-q_\perp^2 R_\perp^2 - q_\parallel^2 R_\parallel^2 - q_0^2\tau^2)/2\}] , \quad (1)$$

where $q_\perp$, $q_\parallel$ are projections of the relative two-pion momentum $\mathbf{q} = (\mathbf{p}_1 - \mathbf{p}_2)$ perpendicular and parallel to the beam axis, q_0 is the energy difference $|E_1 - E_2|$, and B is a normalization factor. The experimental correlation function is the ratio of the two-pion probability $N_2(\mathbf{p}_1, \mathbf{p}_2)$ to the product of single-pion probabilities $N(\mathbf{p})$:

$$C(\mathbf{p}_1, \mathbf{p}_2) = \frac{N_2(\mathbf{p}_1, \mathbf{p}_2)}{N(\mathbf{p}_1)N(\mathbf{p}_2)} . \quad (2)$$

The Coulomb interactions between the pions and the nuclear fragments, and between the pions themselves, were taken into account as described by Chacon *et al.* [36]. In Ref. [36], however, there was no tag counter array for biasing the data sets toward different mixes of central and peripheral collisions. An average impact parameter had to be assumed, dividing the nuclear charge into three groups at target (20% of the charge), central (60%), and projectile velocities (20%). The data near

TABLE I. Field values for the spectrometer magnets.

Setup	Janus magnet (kG)	"C"-magnet (kG)
0°	10.5	13.2
45°	7.8	0.9

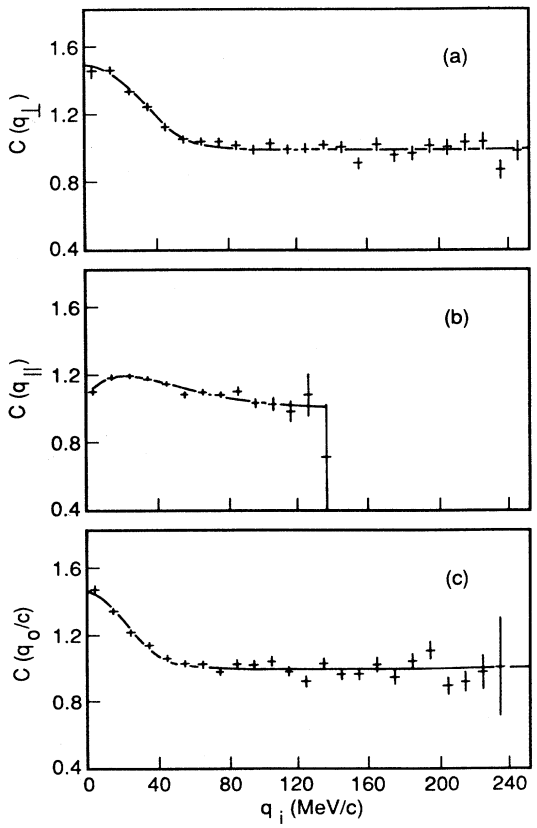

FIG. 2. Experimental 45° data and correlation function fits for different projections: (a) $C(q_\perp)$, (b) $C(q_\parallel)$, and (c) $C(q_0/c)$.

TABLE II. Fit results of the 0° data for different projectiles with $|\mathbf{p}_{\mathrm{proj}}| > 50$ MeV/c. The results for Ar, Fe, and Nb are taken from Chacon *et al.* [36].

	0° data, $\lvert\mathbf{p}_{\mathrm{proj}}\rvert > 50$ MeV/c			
Projectile	Ar	Fe	Nb	La
$R_\perp$ (fm)	4.8 ± 0.3	4.8 ± 0.2	5.1 ± 0.2	5.3 ± 0.3
$R_\parallel$ (fm)	4.2 ± 0.4	2.7 ± 0.3	4.4 ± 0.3	3.7 ± 0.7
τ (fm/c)	$1.1^{+1.4}_{-1.1}$	2.7 ± 0.6	3.9 ± 0.4	4.7 ± 0.9
λ	0.81 ± 0.06	0.88 ± 0.03	1.11 ± 0.03	1.08 ± 0.06
χ^2/NDF	581/537	939/729	1144/1087	1224/1113
χ^2_{PML}/NDF	2979/2590	2938/2420	3776/3235	4344/4277
Events	12 900	32 000	49 400	28 000

90° (in the c.m.) are rather insensitive to the Coulomb correction, since the momentum difference of a pion pair changes very little. Pions near the beam velocity are more sensitive to this correction. In the La + La case analyses were run using different tag array multiplicity cuts, with various fireball model target, central, and projectile charge divisions, and exclusion limits of 50 MeV/c or 250 MeV/c away from the beam velocity. With the 50 MeV/c exclusion, the different charge divisions did not give results that differed significantly from each other, and the results are expected to be less sensitive to the charge division for the 250 MeV/c exclusion.

Final-state pion-pion hadronic interactions are expected to be small [17], and therefore are not considered in the analysis. Details of the track-finding and data-reduction procedures are given by Chacon [31]. The laboratory momenta of the pion pairs analyzed were in the range 300 to 900 MeV/c in the 0° acceptance, and 150 to 1000 MeV/c in the 45° acceptance. The final data sample consisted of 28 000 (38 500) pion pairs for the 0°(45°) measurement. For this symmetric system the source-size analysis was carried out in the center-of-mass frame.

The reference sample, i.e., the single-pion momentum distribution of Eq. (2) with no Bose-Einstein correlations, was generated using the event-mixing method [26, 31]. To remove the residual correlation in the "mixed-event" sample, correlation function parameters [in Eq. (1)] from a previous fit were taken, and used to generate (by event weighting) a reference sample with the residual correlation effect removed [26, 31]. This reference sample was used to generate a new set of parameters by fitting the correlation function to experimental data. These steps were repeated until the fit results were stable, which was usually the case after 3–5 iterations. In Fig. 2 different projections of experimental data and correlation function fits are shown for the 45° measurement. The differences in shape between the correlation function used in the fit [Eq. (1)] and the projections are due to the acceptance weighting of the projections [36]. No significant deviations from the simple Gaussian source model are evident, such as higher-energy pp studies [35] have observed and attributed to heavier mesons beyond the production energy of the Bevalac.

IV. RESULTS AND DISCUSSION

The dependence of the source parameters on the projectile mass number A for the 0° and 45° configurations is given in Tables II and III, respectively, and is shown in Figs. 3(a) and 3(b). Previous results for Ar, Fe, and Nb have been taken from Chacon *et al.* [30, 36]. The χ^2 given here is restricted so that more than five counts were required in a bin for it to be included in the calculation. The χ^2_{PML} is a χ^2 based on the log-likelihood function used in the principle of maximum likelihood fit, and reduces to the usual χ^2 for sufficient statistics [26, 31]. NDF is the number of degrees of freedom.

For both observation angles the source exhibits an oblate shape ($R_\perp > R_\parallel$) except in the case of Nb for which the source is nearly spherical. The parameter $R_\perp$ is fairly constant over the whole mass range at about 5.0 fm (0°) and 4.5 fm (45°). The lifetime τ strongly increases with the mass number, whereas the chaoticity λ seems to be increasing only in the 0° data. Note

TABLE III. Fit results of the 45° data for different projectiles with $|\mathbf{p}_{\mathrm{proj}}| > 50$ MeV/c. The results for Ar, Fe, and Nb are taken from Chacon *et al.* [36].

	45° data, $\lvert\mathbf{p}_{\mathrm{proj}}\rvert > 50$ MeV/c			
Projectile	Ar	Fe	Nb	La
$R_\perp$ (fm)	4.5 ± 1.0	4.0 ± 0.65	4.8 ± 0.55	4.5 ± 0.75
$R_\parallel$ (fm)	1.0 ± 1.0	$1.5^{+0.55}_{-0.9}$	3.8 ± 0.2	3.6 ± 0.4
τ (fm/c)	$0.0^{+2.3}_{-0.0}$	1.7 ± 1.7	4.8 ± 1.0	7.6 ± 1.0
λ	0.72 ± 0.10	0.66 ± 0.06	0.89 ± 0.035	0.70 ± 0.04
χ^2/NDF	138/156	381/403	846/795	561/541
χ^2_{PML}/NDF	1702/1662	2194/1925	2612/2098	1958/1603
Events	3300	8400	39 100	38 500

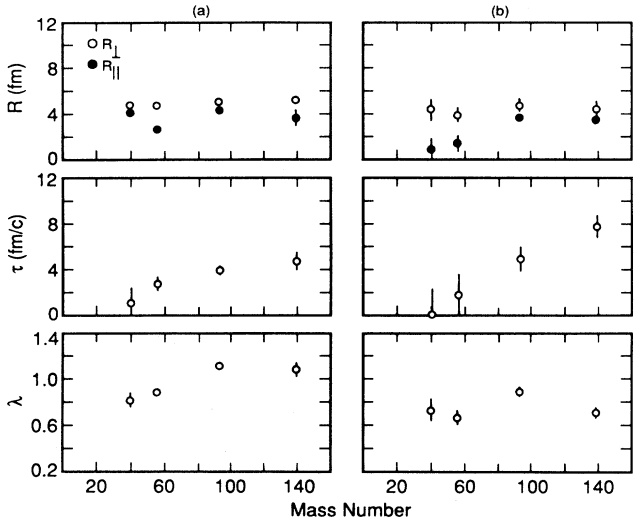

FIG. 3. Gaussian source shape parameters as a function of the mass number of the projectile (= target) for (a) 0° and (b) 45° measurements.

that in the 0° configuration measurements λ approaches the value of 1, corresponding to a completely chaotic source. The general trend in the 45° data seems to indicate a chaoticity parameter of around 0.7. This is in disagreement with nuclear cascade calculations [15] and the "final-state shadowing" effect [8] which both predict λ values around or greater than unity. Fowler and Weiner [13] attribute the lower chaoticity to an increase in stimulated emission through Δ decay along the longer $R_\perp$ axis.

The distribution of the charged-particle multiplicity from the multiplicity array is shown in Fig. 4 for the 45° data. The average number of hits in the array for both viewing angles is about three. The analysis of various tag multiplicity cuts was carried out in the same way for the 0° and 45° data. As mentioned in Sec. II it was not possible to use the tag information from all the scintillators within the full array. Despite periodic changing of the mid-array scintillators struck by the beam, there were radiation-damage effects and high-count-rate effects that precluded their use in the final analysis.

TABLE IV. Average detected multiplicity in the tag array as a function of impact parameter, from FREESCO and GEANT simulations of the experiment. The impact parameter is given in units of the nuclear diameter (e.g., b/b_{max}).

0° setup	
Impact parameter	Average detected multiplicity
0.1	2.2
0.3	4.6
0.5	7.3
0.7	5.6
0.9	2.4
45° setup	
Impact parameter	Average detected multiplicity
0.1	2.5
0.3	5.6
0.5	9.7
0.7	6.6
0.9	1.8

To determine the correlation between tag multiplicity and impact parameter, the FREESCO cascade-coalescence code of Fai and Randrup [39] was used to generate simulated events for different impact parameters. The tag array geometry and magnetic fields were incorporated in the GEANT [40] simulation code with the input of FREESCO events. At first, as Table IV shows, the tag array multiplicity (using 100 simulated events for each

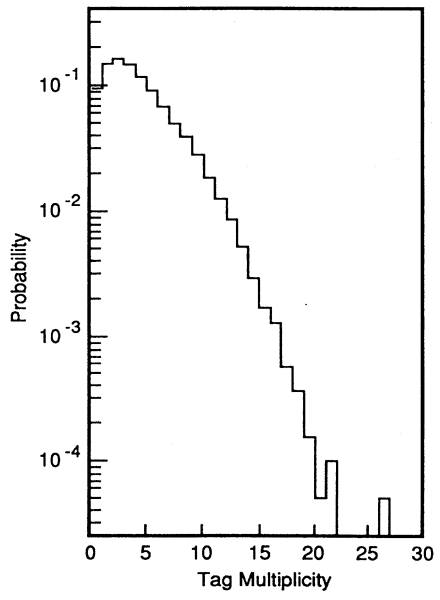

FIG. 4. Distribution of the charged particle multiplicity detected by the multiplicity array for 45° data.

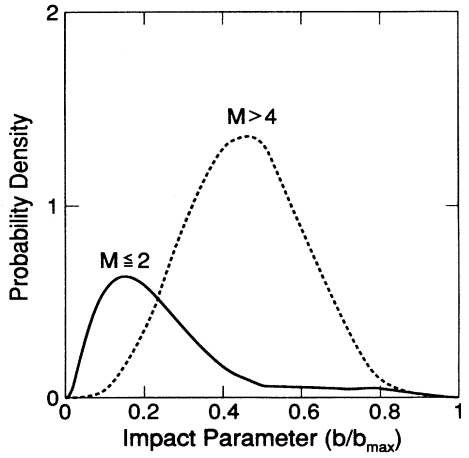

FIG. 5. Probability density as a function of impact parameter for two multiplicity cuts in the tag array.

impact parameter) appears to be of little value, as the impact parameter is a double-valued function of the multiplicity. Obviously the multiplicity is low for the most peripheral collisions, but it is also low for the most central collisions since these violent central collisions throw most of the charged particles to wider angles than the 5.5° subtended by our array. However, the events measured have two negative pions detected in the Janus spectrometer, and this strongly biases the events toward central collisions because of the spectrometer's small acceptance.

Another program was used to fold together the tag array multiplicity, Poisson statistics, and the two-pion trigger probability. The simulated tag array multiplicity was scaled downward somewhat to reproduce the observed average multiplicity. The calculated impact-parameter distributions for two tag multiplicity cuts are shown in Fig. 5. The pion production probability has suppressed the large impact parameters so that the multiplicity is now a positive monotonic, if broad, measure of the impact parameter. Note that the relationship between the detected multiplicity and the centrality of the collision is reversed from that of a 4π detector — larger detected multiplicity is less central and smaller detected multiplicity is more central.

For the 0° data, the selection of two-pion events according to multiplicity does not have a statistically significant effect on the source parameters, as demonstrated in Fig. 6(a) and Table V. The various cuts on the multiplicity in the array (M) are indicated, along with the unbiased data ("unbd"). In contrast to the 0° data, the requirement of low multiplicities in the 45° data causes the source shape to become more oblate, and the selection of high multiplicities leads to almost spherical source shapes [see Fig. 6(b) and Table VI]. In an attempt to extract a set of peripheral collisions, the zero-hit condition was relaxed to also include events that had pulse-height overflows, the idea being that heavy beam residues either passed (undetected) through the center of the multiplicity array or caused an overflow in the innermost ring of counters (this condition is denoted "M=$\emptyset OF$" in Fig. 6, and in Tables V and VI). Since FREESCO does not generate heavy fragments (only coalescence fragments up to mass $\approx$ 30), it is not possible to have confidence in the impact-parameter selection of the condition $M = \emptyset OF$.

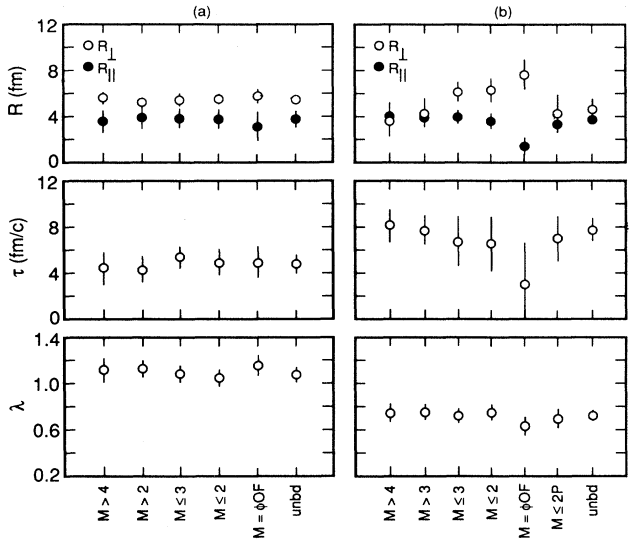

FIG. 6. Gaussian source shape parameters for different multiplicity requirements on (a) 0° and (b) 45° data. Results with no multiplicity requirements are labeled "unbd" (for unbiased), and the zero multiplicity condition "$M = \emptyset OF$" is explained in the text. The data set labeled "$M \leq 2P$" shows the effect of a projectile-frame momentum cut ($|\mathbf{p}_{\rm proj}| > 250$ MeV/c rather than the usual cut of $|\mathbf{p}_{\rm proj}| > 50$ MeV/c) on a $M \leq 2$ multiplicity data sample.

It is inherently difficult to simultaneously determine τ and the size parameter along the line of observation, and many confidence contour plots were presented in Ref. [36]. The uncertainties quoted take the usual conservative estimate [41] from the confidence contour plots. The uncertainties shown in Fig. 6 take into account the correlation of the components of R and the lifetime τ. Thus, the finite value reported for τ is statistically significant, and with the large number of events within a small solid angle it is not necessary to force τ to zero, as in some earlier streamer-chamber studies.

TABLE V. Source parameters for the 0° measurement with varying biases imposed through multiplicity cuts. For an explanation of the symbols, see the text.

		0° data		
Class	$M > 4$	$M > 2$	$M \leq 3$	$M \leq 2$
$R_\perp$ (fm)	5.6 ± 0.5	5.2 ± 0.4	5.5 ± 0.5	5.4 ± 0.4
$R_\parallel$ (fm)	3.6 ± 1.1	3.8 ± 0.8	3.9 ± 0.9	3.7 ± 0.9
τ (fm/c)	4.5 ± 1.4	4.3 ± 1.2	5.4 ± 1.0	4.9 ± 1.1
λ	1.12 ± 0.10	1.12 ± 0.08	1.08 ± 0.08	1.06 ± 0.08
Class	$M = \emptyset OF$	unbd		
$R_\perp$ (fm)	5.6 ± 0.5	5.3 ± 0.3		
$R_\parallel$ (fm)	3.2 ± 1.3	3.7 ± 0.7		
τ (fm/c)	4.9 ± 1.4	4.7 ± 0.9		
λ	1.16 ± 0.11	1.08 ± 0.06		

TABLE VI. Source parameters for the 45° measurement with varying biases imposed through multiplicity cuts. For an explanation of the symbols, see the text.

		45° data		
Class	$M > 4$	$M > 3$	$M \leq 3$	$M \leq 2$
$R_\perp$ (fm)	3.5 ± 1.4	4.1 ± 1.2	5.9 ± 0.9	6.1 ± 1.0
$R_\parallel$ (fm)	3.8 ± 0.6	3.7 ± 0.5	3.8 ± 0.5	3.4 ± 0.5
τ (fm/c)	8.0 ± 1.6	7.6 ± 1.4	6.7 ± 2.1	6.4 ± 2.3
λ	0.74 ± 0.07	0.76 ± 0.06	0.72 ± 0.06	0.74 ± 0.07
Class	$M = \emptyset OF$	$M \leq 2P$	unbd	
$R_\perp$ (fm)	7.4 ± 1.3	4.0 ± 1.6	4.5 ± 0.8	
$R_\parallel$ (fm)	1.3 ± 0.8	3.2 ± 0.6	3.6 ± 0.4	
τ (fm/c)	$3.0^{+3.6}_{-3.0}$	6.9 ± 1.9	7.6 ± 1.0	
λ	0.62 ± 0.08	0.67 ± 0.07	0.70 ± 0.04	

Comparing the $M > 4$ (less central) and $M \leq 2$ (most central) parameter sets in Fig. 6, the 0° pion data show almost no impact-parameter dependence, with a moderately oblate source shape and a chaoticity parameter λ near unity. On the other hand, the 45° (laboratory) pion data have an oblate source shape for the most central and a spherical source shape for the intermediate impact parameters. (There is no information in this data set on very peripheral reactions.) Neither τ nor λ show any significant dependence on impact parameter.

As discussed in Sec. III, it was verified that the multiplicity dependence in the 45° data is not an artifact of the Coulomb correction. However, demanding that the pions have a projectile frame momentum greater than 250 MeV/c leads to a nearly spherical source shape, similar to the unbiased one. This case is shown for multiplicity $M \leq 2$ in Fig. 6 and in Table VI (denoted "$M \leq 2P$"). Thus these 90° c.m. more central events have their most energetic pions showing a spherical source and those between 50 MeV/c and 250 MeV/c in the projectile frame showing an oblate source. This puzzling behavior might be a hint for future theoretical studies to pay attention to side-splash and moving-source effects [11].

The multiplicity dependence of source radii determined by two-particle correlation measurements has been investigated earlier by others. In Refs. [29, 32, 35] no such multiplicity dependence has been found, whereas Refs. [22–25, 27, 33] report an increase of the radius with increasing multiplicity (centrality) of a collision.

Our downstream array had insufficient solid angle to establish a reaction plane. Future studies might aim at measurements of the three radius parameters of an ellipsoidal source with respect to the reaction plane. The question of pion rescattering might then be better resolved.

V. SUMMARY

In this study we extended the determination of space-time dimensions of pion sources in symmetric heavy-ion collisions using Bose-Einstein correlations to the higher mass system ^{139}La. As in previous measurements, the radius perpendicular to the beam axis has been found to be larger than the radius in the beam direction. Our results do not follow an $A^{1/3}$ dependence of the radii on the mass of the projectile [42] but are nearly constant. The chaoticity parameter λ shows only small variations with the projectile mass, whereas the lifetime increases for heavier projectiles. For the 0° observation angle the source shows almost completely chaotic behavior ($\lambda \approx 1$), and at the 45° (90° c.m.) angle the chaoticity is reduced ($\lambda \approx 0.7$). The tag multiplicity dependence of the 90° c.m. data is puzzling, and the fit parameters for the 0° data are independent of the tag multiplicity. Perhaps these results can be a guide for analysis of next-generation heavy-ion pion interferometry experiments using time projection chambers.

ACKNOWLEDGMENTS

The skilled efforts of the Bevalac staff to provide a stable beam are gratefully acknowledged. We appreciate discussions with G. Batko and S. Pratt regarding theory and modeling, including G. Batko's preliminary BUU cascade-code results. This work was supported by the Director of Energy Research, Division of Nuclear Physics of the Office of High Energy and Nuclear Physics of the U.S. Department of Energy under Contracts No. DE–FG03–87ER40323, No. DE–FG05–88ER40437, and No. DE–AC03–76SF00098.

[1] G. Goldhaber, W. B. Fowler, S. Goldhaber, T. F. Hoang, T. E. Kalogeropoulos, and W. M. Powell, Phys. Rev. Lett. **3**, 181 (1959).

[2] G. Goldhaber, S. Goldhaber, W. Lee, and A. Pais, Phys. Rev. **120**, 300 (1960); see also G. Goldhaber, in *Proceedings of the First International Conference on Local Equilibrium on Strong Interaction Physics*, edited by P. Scott and R. Wiener (World Scientific, Singapore, 1985).

[3] G. I. Kopylov and M. I. Podgoretskii, Yad. Fiz. **15**, 392 (1972); **18**, 656 (1973); **19**, 434 (1974) [Sov. J. Nucl.

Phys. **15**, 219 (1972); **18**, 336 (1974); **19**, 215 (1974)]; G. I. Kopylov, Phys. Lett. **50B**, 472 (1974).
[4] E. V. Shuryak, Phys. Lett. **44B**, 387 (1973).
[5] G. Cocconi, Phys. Lett. **49B**, 459 (1974).
[6] F. B. Yano and S. E. Koonin, Phys. Lett. **78B**, 556 (1978).
[7] M. Gyulassy, S. K. Kauffmann, and L. W. Wilson, Phys. Rev. C **20**, 2267 (1979).
[8] M. Gyulassy, Phys. Rev. Lett. **48**, 454 (1982).
[9] J. D. Bjorken, Phys. Rev. D **27**, 140 (1983).
[10] S. Pratt, Phys. Rev. Lett. **53**, 1219 (1984).
[11] S. Pratt, Phys. Rev. D **33**, 72 (1986).
[12] S. Pratt, Phys. Rev. D **33**, 1314 (1986).
[13] G. N. Fowler and R. M. Weiner, Phys. Rev. Lett. **55**, 1373 (1985).
[14] K. Kolehmainen and M. Gyulassy, Phys. Lett. B **180**, 203 (1986).
[15] T. J. Humanic, Phys. Rev. C **34**, 191 (1986).
[16] T. Matsui, Nucl. Phys. **A461**, 27c (1987).
[17] M. G. Bowler, Z. Phys. C **39**, 81 (1988).
[18] G. Bertsch, M. Gong, and M. Tohyama, Phys. Rev. C **37**, 1896 (1988).
[19] B. Lörstad, Int. J. Mod. Phys. A **4**, 2861 (1989).
[20] S. S. Padula, M. Gyulassy, and S. Gavin, Nucl. Phys. **B329**, 357 (1990).
[21] M. Deutschmann *et al.*, Nucl. Phys. **B103**, 198 (1976); **B204**, 333 (1982).
[22] S. Y. Fung, W. Gorn, G. P. Kiernan, J. J. Lu, Y. T. Oh, and R. T. Poe, Phys. Rev. Lett. **41**, 1592 (1978).
[23] J. J. Lu, D. Beavis, S. Y. Fung, W. Gorn, A. Huie, G. P. Kiernan, R. T. Poe, and G. VanDalen, Phys. Rev. Lett. **46**, 898 (1981).
[24] D. Beavis, S. Y. Fung, W. Gorn, A. Huie, D. Keane, J. J. Lu, R. T. Poe, B. C. Shen, and G. VanDalen, Phys. Rev. C **27**, 910 (1983); D. Beavis, S. Y. Chu, S. Y. Fung, W. Gorn, D. Keane, R. T. Poe, G. VanDalen, and M. Vient, *ibid.* **28**, 2561 (1983); D. Beavis, S. Y. Chu, S. Y. Fung, D. Keane, Y. M. Liu, G. VanDalen, and M. Vient, *ibid.* **34**, 757 (1986).
[25] T. Åkesson *et al.* (AFS Collaboration), Phys. Lett. **129B**, 269 (1983); **155B**, 128 (1985); Phys. Lett. B **187**, 420 (1987); Z. Phys. C **36**, 517 (1987).
[26] W. A. Zajc *et al.*, Phys. Rev. C **29**, 2173 (1984).
[27] A. Breakstone *et al.*, Phys. Lett. **162B**, 400 (1985); Z. Phys. C **33**, 333 (1987).
[28] T. J. Humanic *et al.* (NA35 Collaboration), Z. Phys. C **38**, 79 (1988).
[29] R. Bock *et al.*, Mod. Phys. Lett. A **3**, 1745 (1988).
[30] A. D. Chacon *et al.*, Phys. Rev. Lett. **60**, 780 (1988).
[31] A. D. Chacon, Ph. D. thesis, University of California, Berkeley 1989; Lawrence Berkeley Laboratory Report No. LBL–28149 (unpublished).
[32] M. Adamus *et al.* (EHS/NA22 Collaboration), Z. Phys. C **37**, 347 (1988).
[33] D. Allasia *et al.* (WA25 Collaboration), Z. Phys. C **37**, 527 (1988).
[34] A. Bamberger *et al.* (NA35 Collaboration), Phys. Lett. B **203**, 320 (1988).
[35] J. L. Bailly *et al.* (NA23, EHS-RCBC Collaboration), Z. Phys. C **43**, 341 (1989).
[36] A. D. Chacon *et al.*, Phys. Rev. C **43**, 2670 (1991).
[37] R. Hanbury-Brown, R. Jennison, and M. Das Gupta, Nature (London) **170**, 1061 (1952); R. Hanbury-Brown and R. Twiss, Philos. Mag. **54**, 663 (1954); Nature (London) **177**, 27 (1956).
[38] G. Bertsch, Nucl. Phys. **A498**, 173c (1989).
[39] G. Fai and J. Randrup, Nucl. Phys. **A404**, 551 (1983).
[40] R. Brun, F. Bruyant, M. Maire, A. McPherson, and P. Zanarini, CERN Report No. DD/EE/84-1, 1986 (unpublished).
[41] F. James, Comput. Phys. Commun. **20**, 29 (1980).
[42] J. Bartke, Phys. Lett. B **174**, 32 (1986); Int. J. Mod. Phys. A **4**, 1319 (1989).